PAPER • **OPEN ACCESS**

Influence of cavitation on the acoustic boundary conditions in water hammer experiments

To cite this article: Sebastian Klein *et al* 2021 *J. Phys.: Conf. Ser.* **1909** 012015

Influence of cavitation on the acoustic boundary conditions in water hammer experiments

Sebastian Klein[1*], Tobias Traudt[1], Michael Oschwald[1]

[1]Institute of Space Propulsion, Langer Grund 74239 Hardthausen, Germany

E-mail: sebastian.klein@dlr.de

Abstract. A water hammer event is created by stopping a flow in a pipeline using a fast closing valve. The pressure is measured at three different positions upstream the valve. Cavitation occurs close to the valve and is detected by vapour pressure in the pipeline. Frequencies in the liquid part of the pipe were measured and statistically evaluated in order to analyse whether cavitation acts as a boundary condition of acoustics.
Without cavitation one side of the pipe is an open end, while the other side is a closed end. In presence of cavitation the cavity should act like an open end due to the high change of acoustic impedance from liquid to gaseous phase. Therefore it is expected that the oscillating behavior is changing from an open/close to an open/open system. The measured frequencies indeed show a change towards an open/open configuration. It is shown that cavitation acts as a boundary condition in this system.

1. Introduction

Stopping a flow by closing a valve rapidly in a fluid system generates a high amplitude pressure wave which leads to acoustic oscillations inside the fluid system. To understand the wave propagation it is highly important to understand the acoustic boundary conditions. Very detailed overview papers about research activities on water hammer in the last century are written by Bergant et al. [1] and Ghidaoui [2], starting from the work of Joukowsky in the late 19th century.

Cavitation occurs if the local pressure fall below the vapour pressure. In water hammer experiments cavitation occurs close to the valve, since pressure amplitudes are largest here. Such tests with an optical access have been performed at the Fast Transient Test Facility (FTTF) at DLR Lampoldshausen by Traudt et al. [3] and Bombardierri et al. [4]. The influence of static pressure and the occurrence of cavitation on the damping of water hammer waves in the same experiment were investigated by Klein et al. [5, 6].

Besides using an optical access it is possible to measure acoustic emissions from bubble collapses to detect cavitation [7]. Another acoustic method is to measure the reflection or scattering of ultrasonic waves on cavitation bubbles [7]. To measure the void fraction of a two-phase flow various methods are under investigation such as measuring the electric capacity and resistance [8, 9], using wire mesh sensors [10] or X-rays [11]. This work aims on cavitation detection using the cavitation itself as a boundary conditions for pressure waves at eigen frequencies in the liquid part of the system. Since the water hammer is created by closing a valve, the flow is forced to stop before the valve.

2. Theory

Stopping a flow in a pipeline by a fast closing valve triggers a pressure wave travelling upstream the pipeline, the so called water hammer phenomenon. The fundamental equation of which is the Joukowsky equation (eq. 1). It describes the rise of pressure ΔP as a function of the density ρ, the speed of sound c and the change in velocity Δv.

$$\Delta P = \rho c \Delta v \tag{1}$$

The speed of sound in a pipeline is calculated by equation 2 using the compressibility K, the modulus of elasticity E, the pipes diameter d and wall thickness e [12].

$$c^2 = \frac{\frac{K}{\rho}}{1 + \left[\left(\frac{K}{E}\right)\left(\frac{d}{e}\right)\right] C_1} \tag{2}$$

The factor $C1$ for thick wall pipe is a function of the pipelines geometry and the Poisson coefficient ν [12].

$$C_1 = \frac{2e}{d}(1+\nu) + \frac{d(1+\nu^2)}{d+e} \tag{3}$$

The wave starts to oscillate in the pipeline. Depending on the boundary conditions the eigen frequencies f can be calculated by the length l, c and the modennumber $n \in \mathbb{R}$. In case of a pipe with an open and a closed end (o/c) equation 4 must be used.

$$f_{oc}(n) = (2n-1) \cdot \frac{c}{4l} \tag{4}$$

In a pipeline open at both ends (o/o) equation 5 is applied where $f_{oo}(n=1)$ is twice the frequency of $f_{oc}(n=1)$, while the frequency difference between the overtones $\Delta f = f(n+1) - f(n)$ is the same: $\Delta f_{oc} = \Delta f_{oo}$.

$$f_{oo}(n) = n \cdot \frac{c}{2l} \tag{5}$$

If the wave hits a different medium it is reflected and transmitted at the boundary between the two media [14]. The reflection coefficient R for vertical incidence of a wave travelling from medium 1 to medium 2 is descibed by Skudrzyk [15],

$$R = \frac{\zeta - 1}{\zeta + 1} \tag{6}$$

where $\zeta = Z_2/Z_1 = \rho_2 c_2/\rho_1 c_1$ is the ratio of impedance Z at the media interface.

Acoustic cavitation occurs in the pipeline if the local pressure is below the vapour pressure P_v. This happens at sufficiently large amplitudes of the pressure oscillation. The gas bubbles can appear in different size and shape as described by Bergant et al. [1].
The density in this two phase area can be calculated by adding the weighted densities.

$$\rho(\chi) = \rho_g \cdot \chi + (1-\chi) \cdot \rho_l \tag{7}$$

The void fraction $\chi = V_g/V_m$ is the proportion of gas volume V_g in total volume of the mixture V_m.
To calculate the speed of sound in a two phase flow c_{2p} equation 8 can be used, which is valid for bubbly flows [13]. The input parameters are density and speed of sound, both in liquid and gaseous phase, as well as the void fraction.

$$\frac{1}{c_{2p}^2} = \frac{(1-\mathcal{X})^2}{c_l^2} + \frac{\mathcal{X}^2}{c_g^2} + \mathcal{X}(1-\mathcal{X})\frac{\rho_g^2 c_g^2 + \rho_l^2 c_l^2}{\rho_l \rho_g c_l^2 c_g^2} \tag{8}$$

As shown in Fig. 1 even a small deviation from pure liquid or pure gaseous results in a massive decrease of c_{2p}. The acoustic impedance in a two phase flow can be found in Fig. 2. Similar to the speed of sound a huge decrease of the impedance is observed for a small amount of gas.

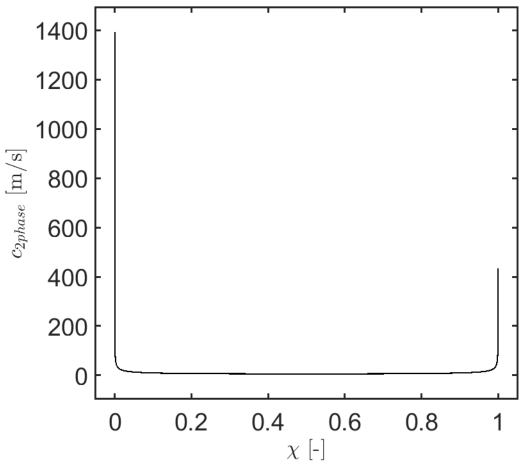

Figure 1. Speed of Sound in a bubbly flow c_{2p} as a function of χ (eq. 8)

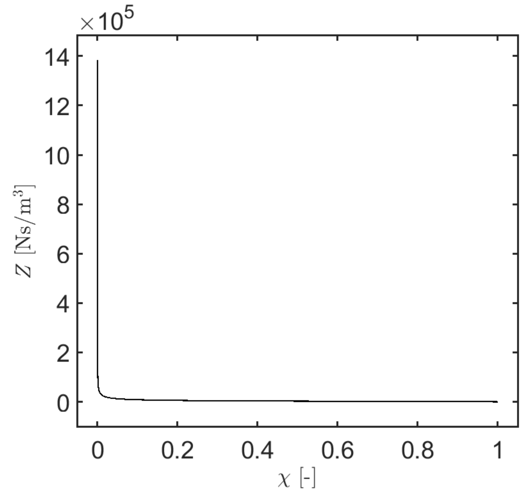

Figure 2. Acoustic impedance as a function of the void fraction χ

2.1. Hypothesis

After a water hammer event a pressure oscillation with a frequency of equation 4 will occur in a pipeline. This configuration is shown in Fig. 3, where l_1 is the length of the pipeline from valve to tank.
The occurrence of cavitation close to the valve is displayed in Fig. 4. In the area of cavitation the impedance is decreasing with respect to Fig. 2. For a wave travelling from the liquid to the cavitation part the reflections coefficient R becomes nearly -1. Therefore the boundary condition on the left is changing from a close to an 'open' end. It is expected that the measured frequencies in the liquid part are matching with frequencies predicted by equation 5. Due to the change of length from l_1 to l_2 higher frequencies are expected.

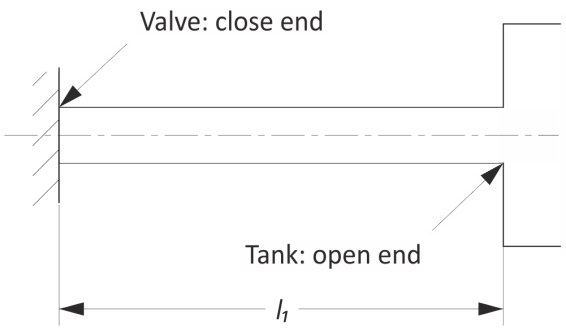

Figure 3. Pipeline with the valve as a closed end and the tank as an open end

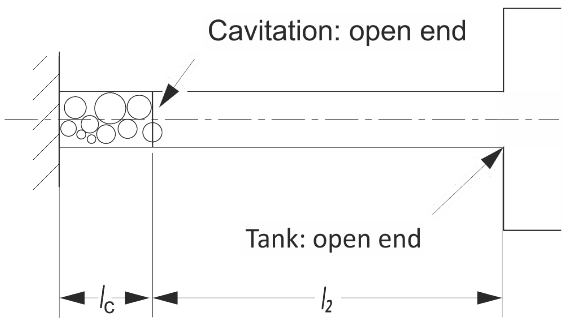

Figure 4. The cavitation in the pipeline acts as an open boundary condition due the impedance change from liquid to two phase area

3. Experiment

The FTTF is shown in Fig. 5. Water flows from the high pressure tank (1) through the pipeline (3) to the low pressure tank (2). The flow rate is measured by the coriolis flow meter (5) and the flow is stopped by the fast closing valve (4). Due to its fast closing time of around $\Delta t_{valve} = 17$ ms the Joukowsky pressure is nearly reached [16]. To calculate the Eigenfrequencies the pipelines

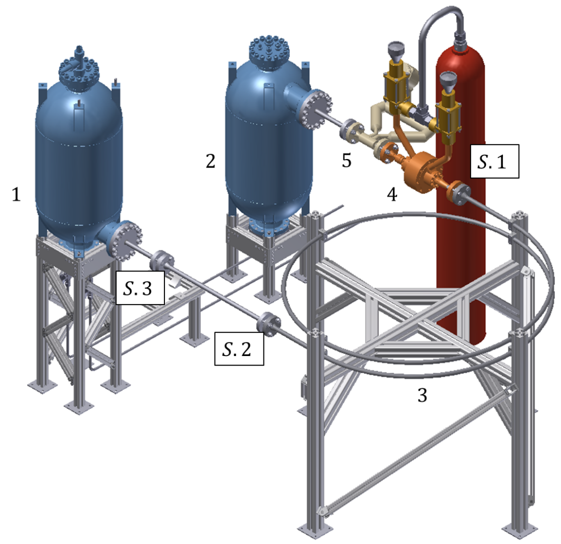

Figure 5. FTTF - Fluid Transient Test Facility, a detailed description can be found in Ref. [5]

1	High pressure tank (HP tank)
2	Low pressure tank (LP tank)
3	Test pipe
4	Fast closing valve
5	Coriolis flow meter
$S1$	Sensor position 1
$S2$	Sensor position 2
$S3$	Sensor position 3

length $l_1 = 7.671$ m and the speed of sound $c_l = 1392$ m/s [16] is required. By using equations 4 and 5 the analytical frequencies for an o/c and o/o system can be calculated. The results are shown in table 1. To create a water hammer the pressure the HP tank is bigger then in the

Table 1. Analytical modes in an o/c and o/o resonator of length l_1 and speed of sound c_l

Mode	o/c	o/o
f_1	45.36	90.731
f_2	136.09	181.46
f_3	226.82	272.19

LP tank $P_{HP} > P_{LP}$. After opening the valve (4) a stationary flow is formed in $\Delta t = 4.6$ s, then the valve is closed and a water hammer is created down- and upstream of the valve. The water hammer is measured upstream of the valve using the sensor positions S1-S3. Each sensor position is equipped with a static pressure sensor P_i (sample frequency $f_s = 1$ kHz), a dynamic pressure sensor $P_{dyn,i}$ ($f_s = 150$ kHz) and a thermocouple.

4. Methods

The pressure trace of the reference case is shown in Fig. 6, the corresponding FFT can be found in Fig. 7. As expected the FFT peaks coincide with the analytical solution for an open close resonator.

To test the hypothesis from section 2.1 pressure oscillations in the liquid part must be measured while cavitation appears close to the valve. In Fig. 8 the pressure traces of the dynamic pressure sensors at position 1 and 2 (P_{dyn1},P_{dyn2}) are shown. The pressure measured by these sensors is relative to P_{HP}. Cavitation is detected by the pressure sensor at position S1 reaching the vapour pressure after the first peak and holding it for $\Delta t_1 = 138$ ms. The pressure measured at S2 does not reach vapour pressure but show oscillations.
S2 is chosen over S3 because the open end leads to a pressure node at the tank. Dissolved gas is

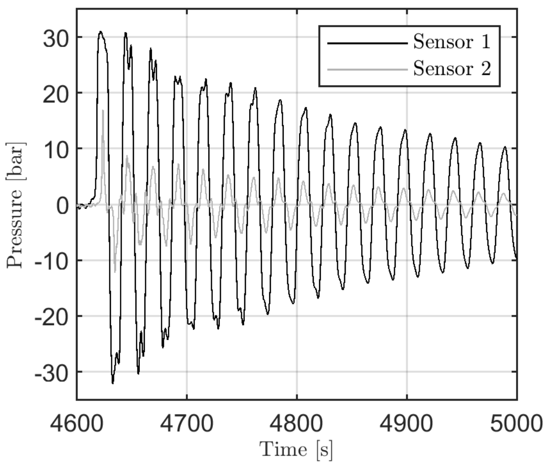

Figure 6. Pressure trace of the reference test case without the occurrence of cavitation.

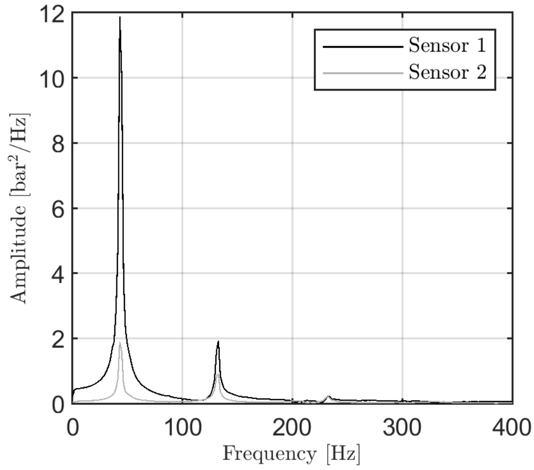

Figure 7. FFT at Sensor 1/2 from $t = 4620 - 5200$ ms in the reference case.

released from water as a result of pressure drop. Since gas absorption is in order of minutes [1], it is assumed that possible released gas remains in the water after the first valley. To exclude effects of released gas in the flow only the first valley is analysed.

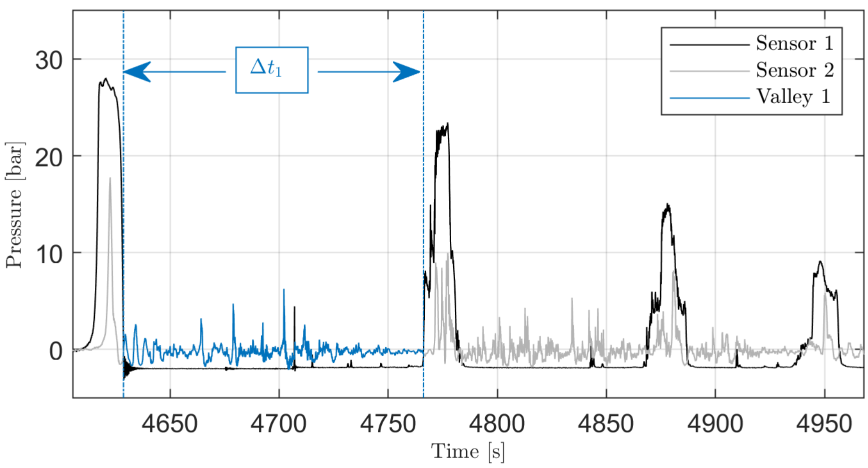

Figure 8. Valley 1 with Cavitation at Sensor 1, no cavitation is measured at Sensor 2

To determine the frequencies in the liquid phase a FFT of $P_{dyn,2}$ of the first valley Δt_1 is done for multiple tests. The FFTs resolution is $\Delta f = 1/\Delta t_1$, to reach $\Delta f = 10$ Hz the minimum valley length is determined to $\Delta t_{1,min} = 100$ ms. For all 75 test cases considered , the three frequency peaks with the highest amplitude of $P_{dyn,2}$ are presented in an histogram in Fig. 9. Error bars are calculated as the square root of m, where m is the number of appearances.

It is assumed that each eigen frequency shows a Gaussian distribution in the histogram, which is described as:

$$g_i(x) = \frac{A_i}{\sqrt{\sigma_i^2 2\pi}} \cdot exp\left(-\frac{(x-\mu_i)^2}{2\sigma_i^2}\right) \tag{9}$$

with a scaling parameter A, the variance σ^2 and the expected value μ. Since two eigen frequencies are expected the following fit function is used:

$$g_{fit}(x) = \sum_{i=1}^{2} g_i(x) \tag{10}$$

5. Verification

In Fig. 9 peaks around $f = 100$ and 200 Hz are visible in the histogram. The fit function g_{fit} (eq. 10) is used to determine the eigen frequencies, which were identified as $\mu_1 = f_1 = 102$ Hz and $\mu_2 = f_2 = 207$ Hz. The other fit parameters are $\sigma_1^2 = 570$, $\sigma_2^2 = 5151$, $A_1 = 613$ and $A_2 = 1524$.

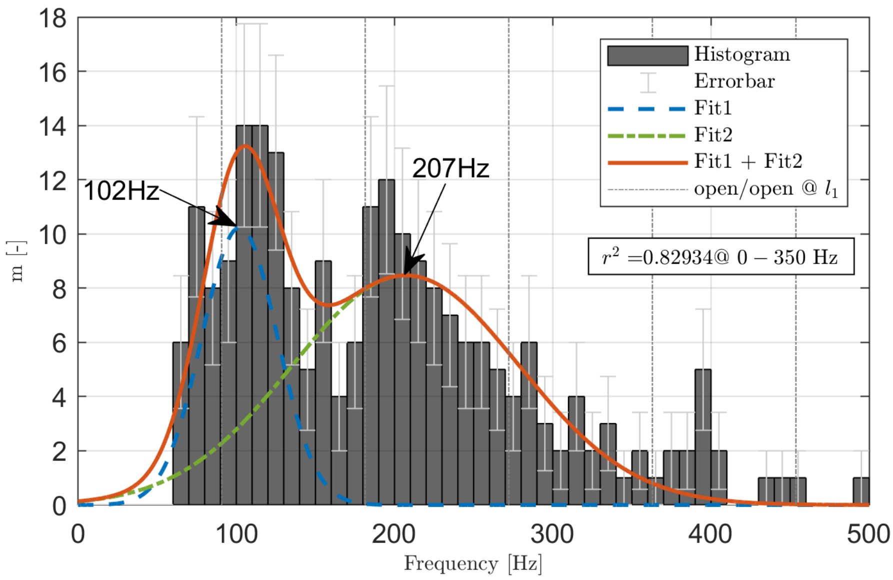

Figure 9. Histogram of the three most excited frequencies in the first valley. The fit function g_{fit} is the sum of two Gauss fits.

A good agreement with the o/o hypothesis is achieved since f_2 is twice as large as f_1. The fit functions coefficient of determination in the area $f = 0 - 350$ Hz is $r^2 = 0.83$. This area is chosen since there are nearly no data for $f > 350$ Hz.

It is of interest how the experimental fit performs against the analytical solutions listed in table 2.

Table 2. Fit parameters

Theory	f_1	f_2
experimental fit	102	207
open/open - l_1	90.7	181.4
open/close - l_1	45.4	136

The measured frequencies show a better matching with the analytical solution for o/o at l_1 than o/c at l_1. Due to the length of cavitation l_c the resonator length shrinks from l_1 to l_2. This results in higher frequencies, which are measured on average 11% higher than the analytical ones. This implies an average reduction of the liquid phase by 11% and therefore an average

length of cavitation of $l_c = 0.85|^{+1,25}_{-2,1}$ m for this specific setup. Only the fit around f_1 is used to calculate l_c.
The length of cavitation is different for each test case and it is expected that the length of cavitation is changing over time. Nevertheless, the measured values show a good agreement with the hypothesis.

6. Summary

A hypothesis was made that cavitation in water hammer experiment acts as a boundary condition for pressure oscillations in the liquid part. Cavitation occurs close to the valve if the vapour pressure is undershot by the water hammer expansion wave. The change of impedance from the liquid to the cavitation part is the reason for the reflection of pressure waves. Even small void fraction leads to an immense decrease of impedance.
To verify the hypothesis several water hammer test at the FTTF at DLR Lampoldshausen have been performed. The pressure was measured at three positions in the test pipe, cavitation was detected close to the pipe. In total 75 tests with a first valley length > 100 ms were taken into account.
While the occurrence of cavitation, the three most excited frequencies in the liquid part were statistically evaluated and displayed in an histogram. It was shown that the distribution of frequencies in all tests considered follows a normal distribution around open/open frequencies for a shortened length of the liquid part. With the presented method cavitation can be detected and localized using only one pressure sensor mounted far away from the cavitation itself.
To improve the analysis a finely meshed sensor matrix or optical access can be used to detect the length of cavitation, which than can be compared with the measured frequencies. It is proposed to build a flow experiment where cavitation occurs controlled by a device and test the hypothesis for a flowing system. For space applications it is of interest to use cryogenic fluids, especially liquid oxygen.

References

[1] Bergant, A., Simpson, A.R., Tijsseling A.S.: *Water hammer with column separation: A historical review*, Journal of Fluids and Structures, 22, 2006, pp.135-171.
[2] Ghidaoui, M., Ming, Z., McInnis, D., and Axworthy, D.: *A Review of Water Hammer Theory and Practice*, ASME, 58, 2005, pp.49-76.
[3] Traudt, T., Bombardieri, C. and Manfletti, C.: *High Speed Imaging of Water Hammer with Column Separation*, 12th Pressure Surge Conference, Dublin, 2015.
[4] Bombardieri, C.: *Experimental Investigation of the Filling Process in Evacuated Spacecraft Propulsion System Feedlines*, Ph.D. Thesis, RWTH Aachen University, 2018.
[5] Klein, S., Traudt, T., Bombardieri, C. and Oschwald, M.: *Influence of static pressure on the damping of pressure waves in rocket engine feed lines*, 13th Pressure Surge Conference, Bordeaux, 2018.
[6] Klein, S., Traudt, T., Bombardieri, C. and Oschwald, M.: *Damping of Water Hammer with Cavitation in Rocket Engine Feed Lines*, 32nd International Symposium on Space Technology and Science, Fukui, 2019.
[7] Teija Koivula and Asko Ellman and M. Vilenius: *Experiences on cavitation detection methods*, Tampere University of Technology, Institute of Hydraulics and Automation, Tampere, 2000.
[8] Yuki Sakamoto and Laura Peveroni and Hiroaki Kobayashi and Tetsuya Sato and Johan Steelant and Maria Rosaria Vetrano: *Void fraction measurement in cryogenic flows. Part I: Design and validation of a void fraction capacitive sensor*, Cryogenics vol. 94, pp.36-44, 2018.
[9] Yuki Sakamoto, Laura Peveroni, Hiroaki Kobayashi, Tetsuya Sato, Johan Steelant, Jean-Marie Buchlin: *Void fraction measurement in cryogenic flows. Part II: Void fraction capacitive sensor performances in chilldown experiments*, Cryogenics vol. 96, pp.25-33, 2018.
[10] Vieira, Ronald and Kesana, Netaji and Torres, Carlos and McLaury, Brenton and Shirazi, Siamack and Schleicher, Eckhard and Hampel, Uwe: *Experimental Investigation of Horizontal Gas-liquid Stratified and Annular Flow using Wire-Mesh Sensor*, Journal of Fluids Engineering vol. 136(12), 121301, 2014
[11] K. Hori, T. Fujimoto and K. Kawanishi, *Development of ultra-fast X-ray computed tomography scanner system*, IEEE Transactions on Nuclear Science, vol. 45, no. 4, pp. 2089-2094, Aug. 1998.
[12] Wylie, E.B. and Streeter V. L.: *Fluid transients*, New York, McGraw-Hill International Book Co., 1978.

[13] Wilson, P. S. and Roy, R.A.: *An audible demonstration of the speed of sound in bubbly liquids*, American Journal of Physics, **76**, 2008, pp.975-981.

[14] Landau, L.D. and Lifschitz E.M.: *Lehrbuch der theoretischen Physik Band VI - Hydrodynamik (german)*, 1986, pp.328-330, ISBN: 3-05-500063-3.

[15] Skudrzyk, E.: *The foundation of acoustics*, 1971, pp.297-299, ISBN: 3-211-80988-0.

[16] Traudt, T., Bombardieri, C. and Manfletti, C.: *Influences on Water Hammer Wave Shape an Experimental Study*, 63. Deutscher Luft- und Raumfahrtkongress, Augsburg, 2014.